The shelterin protein POT-1 anchors *Caenorhabditis elegans* telomeres through SUN-1 at the nuclear periphery

Helder C. Ferreira,[1] Benjamin D. Towbin,[1,2] Thibaud Jegou,[1] and Susan M. Gasser[1,2]

[1]Friedrich Miescher Institute for Biomedical Research, CH-4058 Basel, Switzerland
[2]University of Basel, Faculty of Natural Sciences, CH-4056 Basel, Switzerland

Telomeres are specialized protein–DNA structures that protect chromosome ends. In budding yeast, telomeres form clusters at the nuclear periphery. By imaging telomeres in embryos of the metazoan *Caenorhabditis elegans*, we found that telomeres clustered only in strains that had activated an alternative telomere maintenance pathway (ALT). Moreover, as in yeast, the unclustered telomeres in wild-type embryos were located near the nuclear envelope (NE). This bias for perinuclear localization increased during embryogenesis and persisted in differentiated cells. Telomere position in early embryos required the NE protein SUN-1, the single-strand binding protein POT-1, and the small ubiquitin-like modifier (SUMO) ligase GEI-17. However, in postmitotic larval cells, none of these factors individually were required for telomere anchoring, which suggests that additional mechanisms anchor in late development. Importantly, targeted POT-1 was sufficient to anchor chromatin to the NE in a SUN-1–dependent manner, arguing that its effect at telomeres is direct. This high-resolution description of telomere position within *C. elegans* extends our understanding of telomere organization in eukaryotes.

Introduction

Telomeres form the ends of linear chromosomes and consist of repetitive DNA sequences and their associated binding proteins. These resolve the end replication problem (Szostak and Blackburn, 1982) and protect chromosome ends from DNA damage signaling (Garvik et al., 1995) and chromosome fusion (de Lange, 2009). Perhaps as a consequence of this protection, telomeres often assume a distinct subnuclear localization and show less subnuclear mobility than bulk chromatin (Nagai et al., 2010).

Defined subnuclear telomere localization has been best described in budding yeast, where the 32 telomeres of haploid yeast cells cluster to form 3–8 foci at the nuclear periphery (Palladino et al., 1993; Gotta et al., 1996). This arrangement is functionally significant, as the correct organization of telomeres impacts various aspects of telomere homeostasis, including length regulation, the prevention of inappropriate recombination, and efficient SIR-mediated repression (Schober et al., 2009; Taddei et al., 2009; Ferreira et al., 2011).

Correspondence to Susan M. Gasser: susan.gasser@fmi.ch

B.D. Towbin's present address is Weizmann Institute of Science, Rehovot 76100, Israel.

T. Jegou's present address is Roche Diagnostics GmbH, DE-68305 Mannheim, Germany.

Abbreviations used in this paper: ALT, alternative lengthening of telomeres; IF, immunofluorescence; NE, nuclear envelope; SUMO, small ubiquitin-like modifier; SUN, Sad1p, UNC-84.

What has been less clear is whether peripheral telomere localization is conserved and, if so, whether it uses the same anchoring pathways. In particular, it was unclear whether or not telomere position changes during development or upon terminal differentiation. Here we use FISH to monitor telomere architecture in an animal model, the nematode *Caenorhabditis elegans.* We find that peripheral positioning is conserved in *C. elegans* embryos and that it increases during development. Anchoring requires the conserved Sad1p, UNC-84 (SUN) domain protein SUN-1, the shelterin component POT-1, and the PIAS small ubiquitin-like modifier (SUMO) ligase GEI-17 in early embryos, whereas alternative pathways act in adult tissues.

Results and discussion

C. elegans telomeres localize to the nuclear periphery

To monitor telomere localization in *C. elegans*, we performed DNA FISH experiments using a telomeric repeat probe. This labeling revealed multiple foci within each embryonic nucleus

The Rockefeller University Press $30.00
J. Cell Biol. Vol. 203 No. 5 727–735
www.jcb.org/cgi/doi/10.1083/jcb.201307181

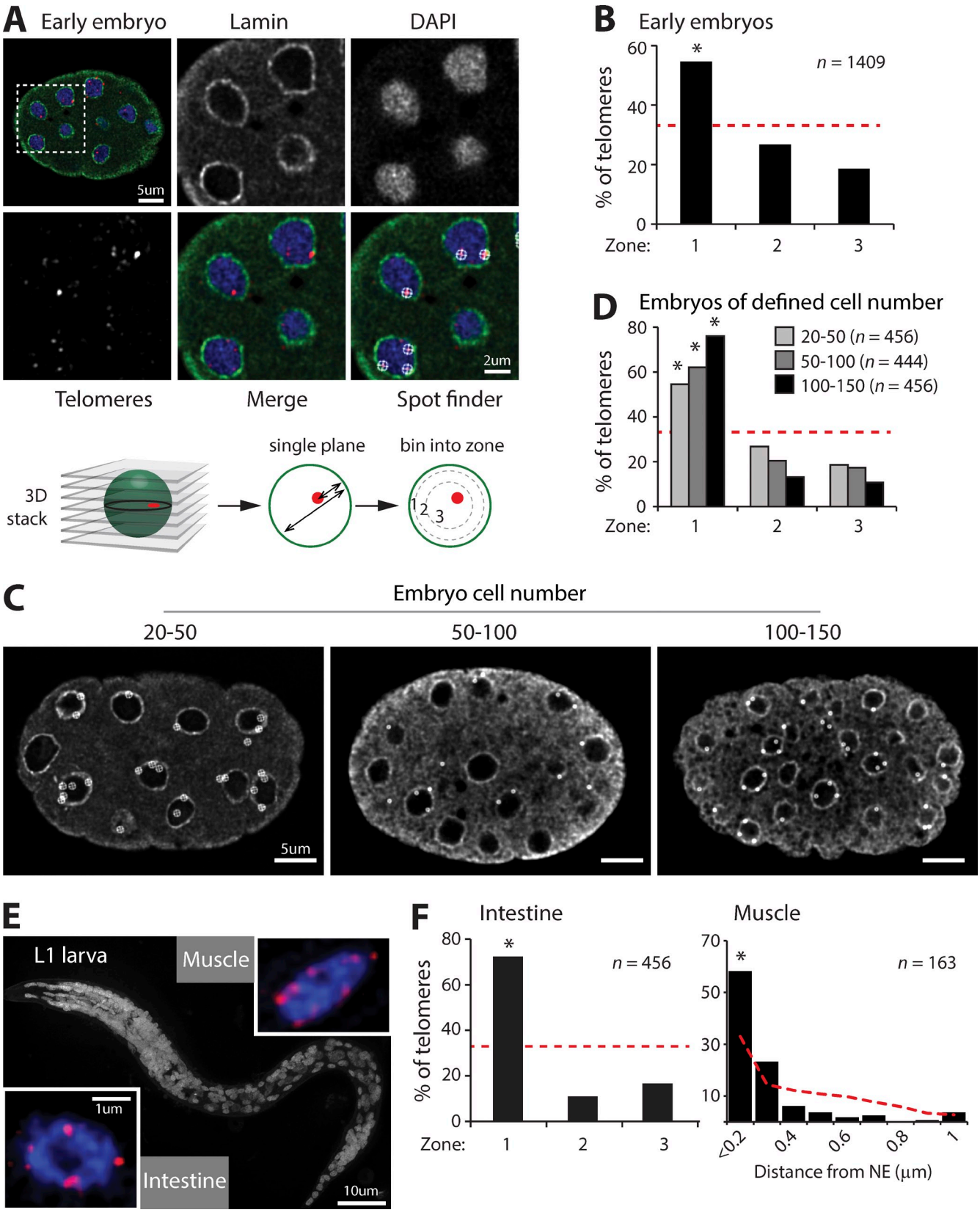

Figure 1. ***C. elegans* telomeres become increasingly peripheral during embryogenesis.** (A) Wild-type N2 *C. elegans* embryos were stained for LMN-1 (Alexa Fluor 488), telomeres (Cy3), and DNA (DAPI) by FISH-IF. A single plane is displayed in the panels. The center of mass of each telomeric focus was determined using the "Spots" function of Imaris. Ratios of the distance from the center of each focus to the nuclear periphery over the nuclear diameter were binned into three concentric zones of equal area, as described in Materials and methods. The boxed region is enlarged in the other panels. (B) Quantification of telomeres in early embryos (20–60 cell stage) shows a significant enrichment at the NE. (C) LMN-1 staining and spot finder–defined telomere foci from a single plane of embryos of increasing age. (D) Quantification of telomere positioning during embryogenesis shows that telomere position becomes

(Fig. 1 A). The punctate signal was sequence-specific, given that FISH performed with a scrambled sequence probe yielded no nuclear foci at all (Fig. S1 A). The punctate signal increased in intensity in mutants with longer telomeres and marked the ends of the highly condensed meiotic pachytene chromosomes (Fig. S1 B). From this we conclude that we can use FISH to visualize telomeres in *C. elegans*.

To determine the radial distribution of telomeres relative to the nuclear periphery, we combined FISH with immunofluorescence (IF) against *C. elegans* lamin (LMN-1; Fig. 1 A). In 3D confocal images, we identified telomere position semiautomatically using commercially available software (Fig. 1 A). Relative position information for these foci was quantified by binning normalized distances from the periphery into three concentric nuclear zones, as described previously (Meister et al., 2010a). In the spherical nuclei of early embryos (20- to 60-cell stage), telomeres were significantly enriched at the nuclear periphery compared with a random nuclear distribution (Fig. 1, A and B). Indeed, telomeres became more peripheral as embryogenesis progressed (Fig. 1, C and D). To test whether this peripheral bias was restricted to embryogenesis, we performed telomere FISH in L1 stage larvae. We found that in at least two postmitotic tissues (muscle and intestine), telomeres were still peripherally enriched (Fig. 1, E and F).

Telomeres become clustered in *C. elegans* ALT-like strains

To assay whether telomeres were clustered, we counted the total number of foci within embryonic nuclei. We observed between 12 and 24 telomeric foci per nucleus (mean of 18.6) in the wild-type N2 strain (Fig. 2 A). Given that *C. elegans* hermaphrodites have 24 telomeres, this suggests that telomere clustering is relatively rare. This mirrors what is normally seen in cycling mammalian cells, which also show little telomere clustering (Nagele et al., 2001). In contrast, extensive clustering of mammalian telomeres into aggregates is observed in cancer cell lines that use the telomerase-independent, alternative lengthening of telomeres (ALT) pathway for chromosome end maintenance (Yeager et al., 1999; Draskovic et al., 2009; Jegou et al., 2009).

ALT-like *C. elegans* strains have recently been described by several laboratories (Cheng et al., 2012; Lackner et al., 2012), allowing us to test how ALT affects telomere architecture. Intriguingly, in four independently generated ALT-like strains, we observed a significant reduction in the number of telomere foci per cell (Fig. 2, B and C; and Fig. S1 C). A *trt-1(ok410) pot-1(tm1620)*–derived ALT-like strain lacking the telomerase catalytic subunit *trt-1* (Meier et al., 2006) had a mean of 2.9 telomere foci per cell (Fig. 2 B), compared to the mean of 18.6 foci observed in wild-type strains. This effect was linked to *trt-1*, as a *pot-1(tm1400)* strain had a wild-type number of telomere foci per cell (Fig. S1 C). A similar reduction in the number of telomere foci per cell (mean of 5.8) was seen in the *mrt-2(e2663); pot-2(tm1400)*–derived ALT-like strain (Fig. 2 C). *mrt-2* is the worm homologue of human RAD1 and is required for *C. elegans* telomerase activity (Ahmed and Hodgkin, 2000). This result argues that worm telomere clustering occurs in the context of ALT due to loss of telomerase activity, rather than loss of the telomerase catalytic subunit. Finally, two additional *trt-1(ok410); unc-29(e193)* strains (c1-25 and c8-25) also showed a reduction in mean telomere number to 12.4 and 9.3, respectively (Fig. 2, D and E).

We explored whether telomere fusions could be responsible for the reduced number of telomere foci observed. However, the number of fusion events seen in *mrt-2; pot-2*– and *trt-1; pot-1*–derived strains (between 0–1 and 1–2 per cell, respectively) are too low to account for this (Cheng et al., 2012). Additionally, the mean telomere lengths in ALT strains are longer than in N2 (Cheng et al., 2012; Lackner et al., 2012). This makes it unlikely that the observed reduction in telomere foci stems from reduced hybridization efficiency. Nonetheless, given that ALT telomeres are heterogeneous in length, we cannot exclude the possibility that we failed to visualize some critically short telomeres. However, the magnitude of the reduction in foci number and the fact that it occurs in an *mrt-2* background, which has more homogeneous telomere length (Cheung et al., 2004), argue that telomere clustering occurs in ALT strains.

Telomeres in ALT cancer cell lines cluster at ALT-associated promyelocytic leukemia (PML) bodies (Yeager et al., 1999). This arrangement is thought to bring telomeres in close proximity to promote telomere–telomere recombination (Potts and Yu, 2007). That we observe telomere clustering specifically in ALT-like *C. elegans* strains indicates that this arrangement may promote telomere maintenance by recombination in worms as well. Interestingly, in all ALT-like *C. elegans* strains monitored, the degree of peripheral telomere localization was less pronounced than in wild-type strains (Fig. 2, B–E). Telomeres in *mrt-2; pot-2* embryos maintained a slight enrichment at the nuclear periphery, but *trt-1; pot-1* telomeres were essentially random (Fig. 2, B and C). This result rules out the possibility that ALT maintenance requires association with the nuclear envelope (NE), and suggests that TRT-1 and/or POT-1 may be involved in anchoring.

SUN-1 and POT-1 are required for telomere localization in embryos

Previous work in yeast had shown that the SUN-domain protein Mps3 anchors telomeres to the nuclear periphery, suppressing short telomere recombination (Bupp et al., 2007; Schober et al., 2009). We therefore tested whether its worm homologue, SUN-1, is similarly involved. Indeed, *sun-1(RNAi)* led to an essentially

increasingly peripheral. (E) FISH was performed on L1 stage larvae. The larger, stitched, image shows a projection of DAPI-stained nuclei. The two inserts show a single plane from either a muscle or intestinal cell; DAPI staining is blue and telomere FISH (Cy3) is in red. (F) Quantification of telomere position in intestinal and muscle cells shows that telomeres are peripherally enriched in both tissues. For intestinal nuclei, the zoning assay was performed as described in B except that the edge of the DAPI signal was used to denote the nuclear periphery. For muscle cells, the absolute distance from the edge of the nucleus is plotted. For all graphs, the red dotted lines denote a hypothetical random distribution. *, $P < 10^{-5}$ compared with random. All images in enlarged panels were scaled sevenfold using bilinear interpolation. All data derive from two or more independent biological replicates.

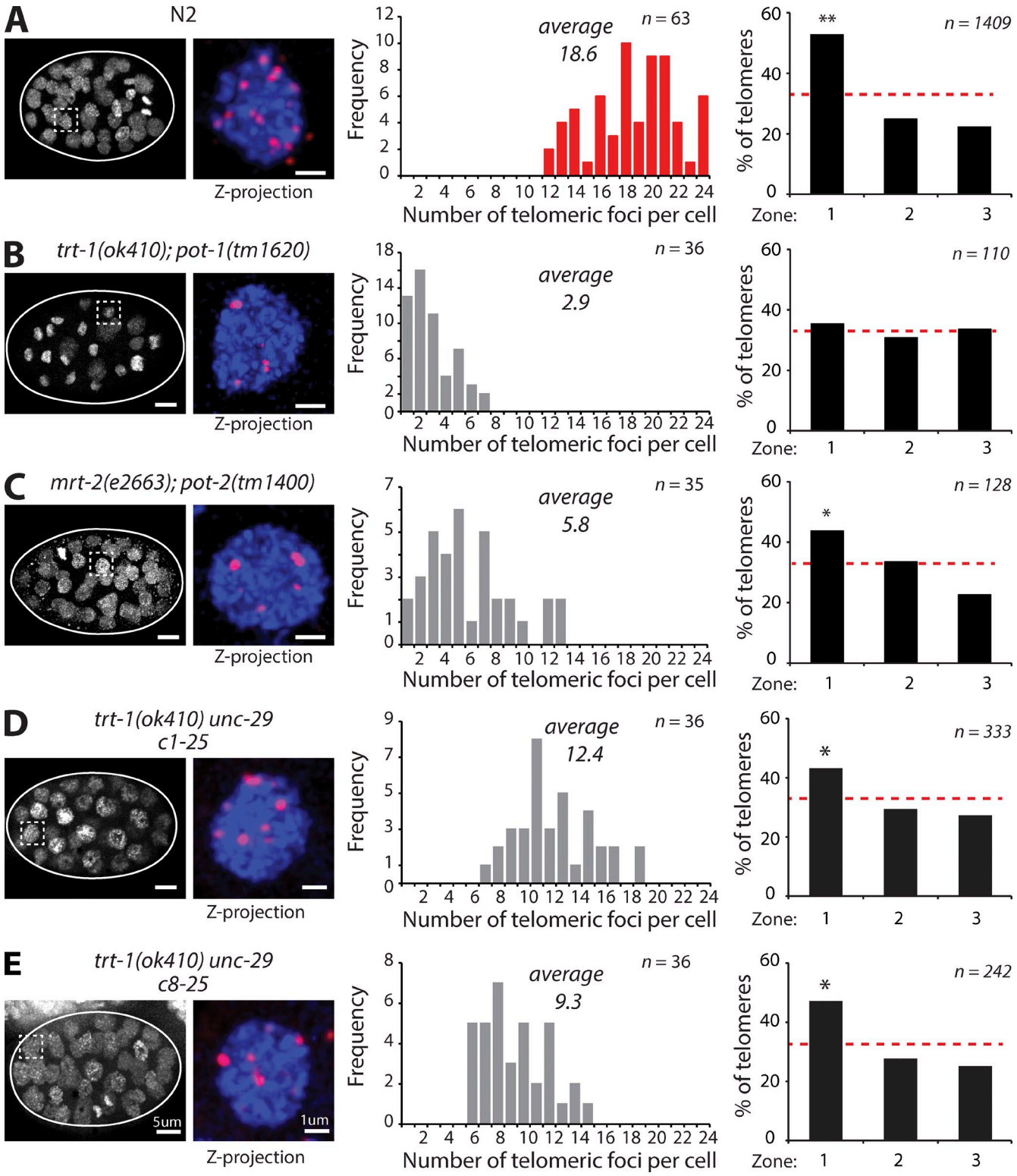

Figure 2. **Telomeres cluster in strains that use ALT.** (A) Telomere FISH-IF was performed as in Fig. 1. The left panel shows a projection of DAPI stained nuclei from a wild-type N2 embryo, the edge of which is outlined in white. The image on the right is an enlargement showing a projection of a single cell with DNA (DAPI) staining in blue and telomere FISH (Atto 647N) in red. Quantification of the number of telomeric foci per nucleus shows a distribution averaging 18.6 foci per cell, which indicates that there is little clustering of telomeres in wild-type embryos. (B) The same procedure was performed in an ALT-like *C. elegans* strain, *trt-1; pot-1*, where a mean of 2.9 foci per cell was observed. (C) This reduction in the number of telomeric foci per nucleus is also observed in another ALT-like strain *mrt-2; pot-2*. (D and E) Two additional ALT-like strains, *trt-1* c1-25 and *trt-1* c8-25, also show fewer telomeric foci per cell (mean of 12.4 and 9.3, respectively). With the exception of *trt-1; pot-1*, ALT-like telomeres are weakly peripheral in embryos. The red dotted lines denote a hypothetical random distribution. *, $P < 10^{-2}$; **, $P < 10^{-5}$ compared with a random distribution. All images in enlarged panels (taken from the boxed regions) were increased in size sevenfold using bilinear interpolation.

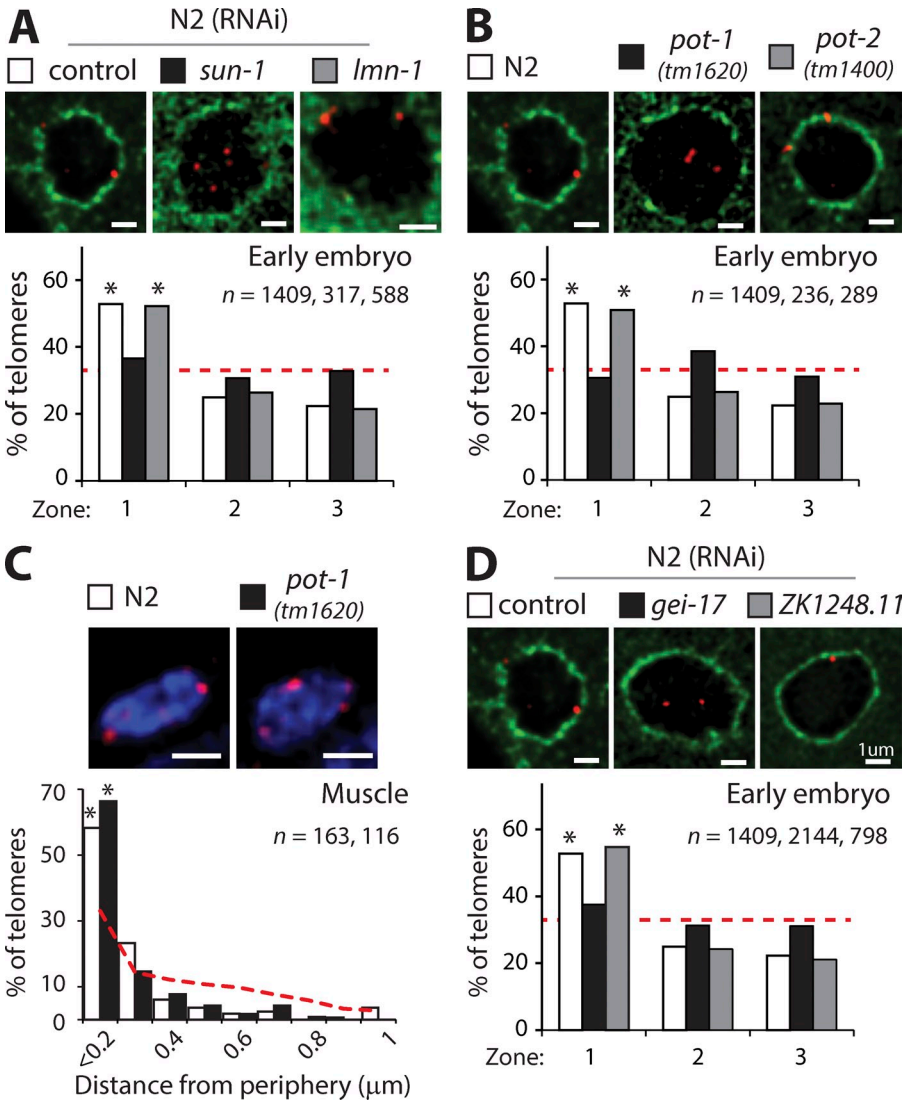

Figure 3. **Telomere anchoring in embryos depends on GEI-17, SUN-1, and POT-1.** (A) RNAi in early embryos (20–60 cell stage) shows that SUN-1 but not LMN-1 anchors telomeres to the NE. Quantification is done as in Fig. 1. A single plane from a representative FISH-IF image is shown; lamin (Alexa Fluor 488) is marked in green and telomeres (Atto 647N) in red. During *lmn-1* RNAi, the nuclear periphery was defined using the edge of the DAPI signal. (B) Telomere anchoring in embryos requires the telomere binding protein POT-1 but not POT-2. (C) Quantifying telomere position in L1 larvae shows that POT-1 is not required for telomere position in postmitotic muscle cells. (D) The PIAS-type E3 SUMO ligase GEI-17, but not the E3 SUMO ligase ZK1248.11, is required for telomere anchoring. The red dotted lines denote a hypothetical random distribution. *, $P < 10^{-5}$ compared with a random distribution. All images were increased in size sevenfold using bilinear interpolation. The experiments shown in A, B, and D were conducted in parallel, and all comparisons are presented relative to the same control image.

random telomere distribution in early embryos (Fig. 3 A). In contrast, down-regulation of the nuclear intermediate filament protein, lamin (LMN-1), had no effect on telomere localization. The efficiency of *lmn-1(RNAi)* was verified by IF against LMN-1 (Fig. S2 A). Given the prevalent roles of lamin in the organization of heterochromatin (Dechat et al., 2008; Gonzalez-Suarez et al., 2009; Mattout et al., 2011), this result was somewhat surprising. However, consistent with our result, the association of SUN-1 with the inner nuclear membrane is LMN-1 independent (Penkner et al., 2007).

In an attempt to identify the telomere binding factor that mediates anchoring, we turned to the DNA end-binding factor Ku, which bridges telomeres to the SUN domain protein, Mps-3 (Laroche et al., 1998; Ebrahimi and Donaldson, 2008; Schober et al., 2009). However, in a *cku-80(ok861)* background, telomeres were still bound to the nuclear periphery (Fig. S2 B). This result is consistent with the fact that deficiency for *cku-80* does not accelerate the senescence phenotype of *trt-1* mutants (Lowden et al., 2008).

The end-protection functions of Ku overlap with the shelterin complex, which binds both double- and single-stranded telomeric repeats to protect telomeres from end-to-end fusions (de Lange, 2009). We therefore tested whether the single-strand DNA (ssDNA) telomere binding proteins POT-1 and POT-2 (Raices et al., 2008; Cheng et al., 2012; Lackner et al., 2012) play a role in telomere anchoring. We found that loss of POT-1, *pot-1(tm1620)*, but not of POT-2, *pot-2(tm1400)*, provoked telomere delocalization in early embryos (Fig. 3 B). This indicated that altered telomere position does not correlate simply with increased telomere length, as the absence of either POT-1 or POT-2 increases telomere length over that of wild-type strains (Raices et al., 2008). Rather, anchoring appears to depend specifically on POT-1, which acts nonredundantly with POT-2 at telomeres (Raices et al., 2008; Cheng et al., 2012; Shtessel et al., 2013).

Given that *pot-1* affects telomere localization and promotes ALT in a *trt-1* background (Lackner et al., 2012; Shtessel et al., 2013), we tested whether telomere localization might affect telomere recombination. We assayed telomere recombination by monitoring the levels of single-stranded telomere circles (C-circles; Henson et al., 2009). However, we found that both *pot-2* and *pot-1* mutants showed a similar increase in C-circle levels, even though only one affected anchoring. Moreover,

sun-1(RNAi), which releases telomeres like loss of *pot-1*, led to only a mild increase in C-circles (Fig. S3). Thus, we find no strict correlation between telomere delocalization and enhanced telomere C-circles, which could represent inappropriate T-loop resolution (Vannier et al., 2012) or activation of specific telomere recombination pathways (Hagelstrom et al., 2010). However, it is not possible to completely exclude the hypothesis that position affects telomere recombination, given that Mps3-mediated suppression of recombination was only detected in sensitized genetic backgrounds in yeast (Schober et al., 2009).

Telomeres remain peripheral in postmitotic nuclei in the absence of POT-1

Single-strand DNA-binding proteins may be especially important during telomere replication, when single-stranded telomere stretches are exposed (Wellinger et al., 1993; Wright et al., 1997), and less relevant in noncycling cells. To see whether POT-1 was involved in telomere anchoring in postmitotic cells, we examined telomere position in differentiated muscle cells within *pot-1(tm1620)* animals. Strikingly, *pot-1* deletion did not delocalize telomeres in the muscle nuclei of L1 larvae (Fig. 3 C). This is analogous to the anchoring of heterochromatic arrays to the periphery in *C. elegans*, which requires histone H3 K9 methylation ($H3K9^{me}$) in embryos, but not in differentiated L1 larval cells (Towbin et al., 2012). As subtelomeric nucleosomes are enriched in $H3K9^{me}$ (Liu et al., 2011), we examined whether this histone mark is required for telomere anchoring. We performed FISH for telomeres in *set-25(n5021) met-2(n4256)* embryos, which lack $H3K9^{me}$, and found that there was no loss of perinuclear telomere anchorage (Fig. S2 B). Thus, telomere anchoring and heterochromatin anchoring appear to use different pathways.

The fact that both telomeres and heterochromatic arrays are peripheral in L1 larvae under conditions that cause their release in early embryos suggests that redundant anchoring pathways arise during development. Alternatively, it may be that replication is required to make chromatin organization more malleable and thus more sensitive to genetic perturbation. It is intriguing that the degree of peripheral telomere localization in embryos is anti-correlated with cell cycle duration (Bao et al., 2008). We note that as embryogenesis progresses and cell cycle duration slows, telomeres become more peripheral and anchoring is less sensitive to single gene ablation.

The SUMO E3 ligase GEI-17 promotes telomere anchoring in embryos

Given that SUN-1 and POT-1 are transcribed in both adults and embryos, we examined whether anchoring was regulated posttranslationally. We turned our attention to SUMO modification, as our previous work had identified the SUMO E3 ligase, Siz2, as a regulator of telomere anchoring in yeast (Ferreira et al., 2011). RNAi knockdown of the *C. elegans SIZ2* homologue, *gei-17*, resulted in delocalization of telomeres from the nuclear periphery (Fig. 3 D). This effect was specific to GEI-17, as RNAi of an unrelated SUMO E3 ligase, *ZK1248.11*, the worm homologue of Mms21/Nse2, had no effect on telomere position (Fig. 3 D). We found that *gei-17(RNAi)* did not delocalize telomeres in muscle nuclei (Fig. S2 C), which confirmed the difference in telomere anchoring between embryos and postmitotic cells reported in Fig. 3 (B and C). We hypothesize that some telomere-associated factors may be sumoylated by GEI-17. Indeed, POT-1 itself contains several SUMO acceptor sites (SUMOplot), although we were unable to detect sumoylated forms of POT-1 in vivo (unpublished data).

POT-1 is sufficient to anchor chromatin at the nuclear periphery through SUN-1

POT-1 is able to bind telomeric DNA (Raices et al., 2008), and it is required to anchor telomeres (Fig. 3 B), yet it cannot be assumed that its role in telomere anchoring is direct. We therefore designed a gain-of-function assay to test whether recruitment of POT-1 is sufficient to anchor chromatin to the nuclear periphery (Fig. 4 A). An array of *lacO* binding sites integrated into the genome was visualized through the expression of GFP-LacI, and we confirmed that it is randomly localized within the nucleus (Fig. 4 B; Meister et al., 2010b). Importantly, when we used a GFP-LacI-POT-1 construct to recruit POT-1 to the array, this array became enriched at the nuclear periphery (Fig. 4 B). We next tested whether the role of POT-1 in anchoring chromatin is dependent on SUN-1 as the peripheral tether. Consistent with this, under conditions of *sun-1(RNAi)*, GFP-LacI-POT-1 was unable to recruit the *lacO* array to the nuclear periphery (Fig. 4 C). The epistasis we observed between these factors in chromatin anchoring suggests that POT-1 and SUN-1 most likely act together to anchor telomeres (Fig. 5 B).

Telomere anchoring in eukaryotes: a conserved phenomenon

This study is the first to define the 3D arrangement of telomeres through *C. elegans* development. We show that *C. elegans* telomeres do not normally cluster in wild-type embryos, although clustering is consistently detected in strains that are dependent on the ALT pathway of telomere maintenance. We find that telomeres in wild-type strains become increasingly associated with the nuclear periphery during embryogenesis (Fig. 5 A). In early embryos, telomere anchoring is dependent on SUN-1 and POT-1, and requires the SUMO ligase GEI-17 (Fig. 5 B). However, additional pathways are likely to exist, as telomeres remain attached to the nuclear periphery in postmitotic cells lacking these components. The enhanced telomere anchoring we observed during development correlates with a general increase in nuclear organization observed in differentiated tissues (Meister et al., 2010b). We propose that telomere anchoring at the nuclear periphery may help to promote general nuclear organization during early development.

Telomeres are found at the nuclear periphery not only in simple eukaryotes such as yeasts (Funabiki et al., 1993; Palladino et al., 1993) and trypanosomes (Chung et al., 1990; DuBois et al., 2012), but also in more complex eukaryotes like plants (Rawlins and Shaw, 1990), flies (Marshall et al., 1996), and, as shown here, worms. The conservation of telomere anchoring across such a wide evolutionary timescale suggests that it may also be relevant in mammals. Recently it was shown that telomeres in human cell lines are transiently associated with the nuclear periphery during postmitotic nuclear assembly

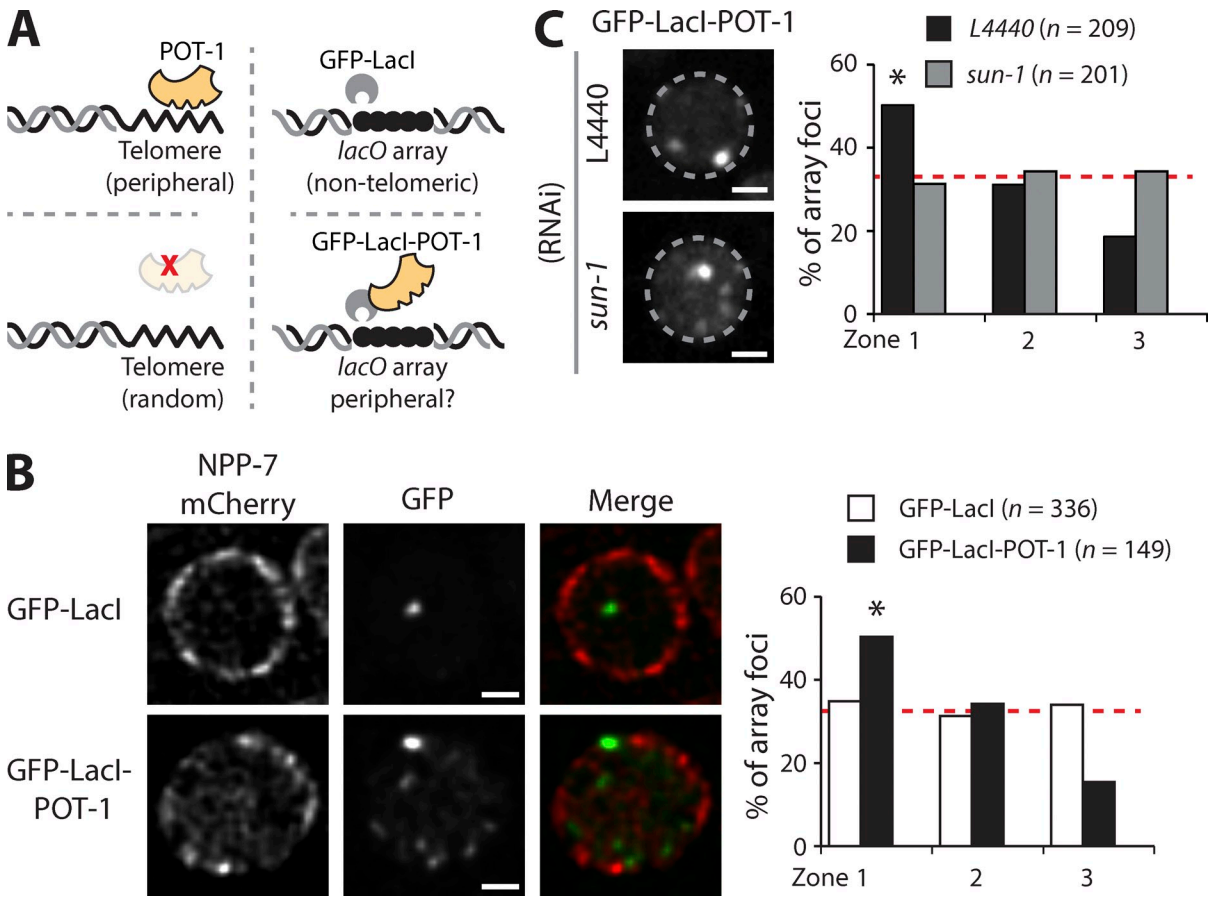

Figure 4. **POT-1 recruitment is sufficient to anchor chromatin.** (A) Experimental scheme to test whether direct recruitment of POT-1 to a nontelomeric locus is sufficient to relocalize it to the NE. (B) The position of an integrated *lacO* array within living embryos was marked by GFP-LacI relative to the NE, marked by NPP-7-mCherry. This is randomly localized but becomes enriched at the NE when GFP-LacI-POT-1 is recruited instead. (C) *lacO* array recruitment to the NE by GFP-LacI-POT-1 is dependent on *sun-1*. Spot position was determined after RNAi for *sun-1*, and for a control (L4440). The nuclear periphery (indicated by the circles) was was determined using background GFP fluorescence. The red dotted lines in the graphs denote a hypothetical random distribution. *, $P < 10^{-5}$ compared with a random distribution. All images were increased in size sevenfold using bilinear interpolation. Bars, 1 µm.

(Crabbe et al., 2012). Strikingly, this depends on SUN1, the human homologue of *C. elegans* SUN-1 and the shelterin subunit, RAP1. As RAP1 knockdown alone did not strongly affect telomere anchoring (Crabbe et al., 2012), additional shelterin subunits such as POT1 may also be relevant. Together these results indicate that telomere anchoring by SUN domain proteins is conserved from worms to man, as well as being important in both mitotic and meiotic cells (Penkner et al., 2007; Starr, 2009). Intriguingly, SUN1 mutation has also been implicated in somatic human disorders (Horn et al., 2013).

Materials and methods

FISH-IF

Embryos from bleached worms were fixed for 5 min in 2% PFA and spread onto poly-L-lysine–coated slides. These were frozen on dry ice before being freeze-cracked and dehydrated for 2 min in 70% (at −20°C), followed by 2 min in 85%, 95%, and 100% ethanol (at 22°C) and then air-dried for 5 min. The slides were washed three times in PBS 0.25% Triton X-100 (PBS-T) for 5 min and blocked in PBS-T 0.5% BSA for 30 min before 1 h of incubation with a 1:1,000 dilution of anti–LMN-1 (rabbit antibody raised against *C. elegans* LMN-1 protein; a gift from Y. Gruenbaum, The Hebrew University of Jerusalem, Jerusalem, Israel) at 22°C. This was washed three

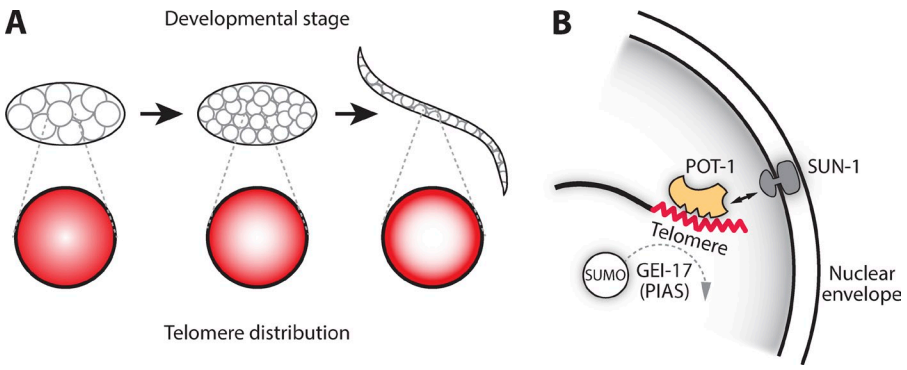

Figure 5. **Model of telomere architecture in *C. elegans*.** (A) *C. elegans* telomeres have a perinuclear bias that increases during embryogenesis and persists in postmitotic tissues. (B) In early embryos, this peripheral bias is dependent on the membrane-associated protein SUN-1, the telomere binding protein POT-1, and the PIAS family SUMO E3 ligase GEI-17. Moreover, POT-1 and SUN-1 are epistatic for chromatin anchoring, and may interact with each other. Given that POT-1 is known to prevent telomere recombination, part of the means by which it does so may be linked to its ability to maintain telomeres at the nuclear periphery.

times with PBS-T before a 30-min incubation with secondary antibody (1:1,000 Alexa Fluor 488 anti–rabbit) at 37°C. The slides were washed three times with PBS-T and then incubated with PBS-T + 1 mg/ml RNase A for 30 min at 37°C, washed again three times with PBS-T, and then post-fixed with 4% PAF in PBS for 10 min at 22°C. Samples were then washed three times in PBS-T and dehydrated for 2 min each in 70% (at −20°C), 85%, 95%, and 100% ethanol (at 22°C) and air-dried for 5 min. 20 µl of the probe mix was placed on the slide, covered with a coverslip, heated to 95°C for 3 min, and left to hybridize overnight at 37°C in a humid chamber. The next day, slides were washed three times for 5 min in 2× SSC with 50% formamide at 39°C and then in 1× SSC for 10 min. DNA was stained in 4× SSC with 0.1 µg/ml DAPI for 5 min at 22°C, washed three times with 2× SSC, and mounted in ProLong Gold antifade (Invitrogen).

Telomere FISH probes were prepared as follows: 40 µl of salmon sperm DNA was ethanol precipitated and resuspended in 160 µl of deionised formamide. Then 2 µl of 10-mM fluorescent DNA probe (Cy3, 5′-TTAGGCTTAGGCTTAGGCTTAGGC-3′) was added. This was heated for 10 min at 72°C, cooled on ice and then mixed with an equal volume of 1:2:2 (20× SSC/50% dextran/10 mg/ml BSA).

Microscopy and analysis

Image acquisition was performed at room temperature on a spinning disk multipoint confocal microscope (IX81 motorized inverted microscope [Olympus], CSU-X1 spinning disc scan head Yokogawa Corporation of America EM-CCD Cascade II camera [Photometrics], and a Plan-Apochromat 100×/1.45 NA oil objective lens) and acquired using MetaMorph 7.7.2 software (Molecular Devices). For live cell imaging, embryos were mounted onto 2% agarose pads surrounded by mineral oil to prevent them from drying out. A z stack covering the embryo with an interval of 0.2 µm was taken and deconvolved using Huygens software (Scientific Volume Imaging). All position analysis was determined from two or more independent experiments and was scored on the number of cells indicated as *n* in each figure.

For Spot finder, the "spots" function of Imaris (Bitplane) was run on images using an estimated spot size of 0.3 µm and with user defined "quality" settings. The marked loci were exported as a TIF file that was loaded into Fiji where the position of each focus relative to nuclear periphery was determined using the PointPicker plugin. The stitching of images to display an entire L1 stage larva (Fig. 1 E) was performed using XuvStitch.

Quantitative analysis of nuclear position in spherical nuclei uses a robust and well-validated method of three-zone scoring (Meister et al., 2010a), which normalizes distance from the periphery to the nuclear diameter in the plane of focus. This has been validated as an accurate method for quantifying position in spherical nuclei of yeast and worms, whereas for aberrantly shaped nuclei (e.g., larval or adult muscle cells), absolute distance to the nuclear periphery must be used (Meister et al., 2010b). In the zoning method, the single plane containing the center of a focus of interest within a 3D stack of images is used. One measures the distance of the focus to the nuclear periphery and the nuclear diameter in that plane. The ratios of distance over diameter for a large number of nuclei are binned into three zones of equal area. To determine whether loci were enriched at the nuclear periphery (zone 1) compared with a random distribution, we applied a χ^2 test (degree of freedom = 2, confidence limit = 95%). In all figures, *n* represents the number of foci analyzed from at least two biological replicates.

C-circle assay

This was performed as described in Henson et al. (2009). In brief, 0.75 µl phi29 polymerase was added to 40 ng of genomic DNA (purified from gravid adults) in a total volume of 10 µl and incubated at 30°C for 8 h. This was spotted onto a neutral Hybond-N membrane, UV cross-linked, and hybridized with a DIG-labeled $(GCCTAA)_4$ probe at 37°C using DIG Easy Hyb (Roche) according to the manufacturer's instructions. As a control the complementary probe was used (Fig. S3).

C96-positive C-circles were created by circularizing the 96-mer oligonucleotide 5′-CCCATATCACTAA$(GCCTAA)_{12}$CCTCAATTCCC-3′ using linker 5′-TGATATGGGGGGAATTGA-3′ as described in Henson et al. (2009) and Shtessel et al. (2013). In brief, the two were mixed in equimolar amounts, heated to 100°C, and left to cool slowly to hybridize. This was then ligated with T4 ligase, and ExoI added to degrade unligated primers.

Strains and confirmation of RNAi efficiency

Strains, including all deletion mutants used in this study, are listed in Table S1. All worms were grown at 20°C. RNAi by bacterial feeding was performed on plates at 22.5°C as described previously (Timmons et al., 2001). Knockdown of LMN-1 was verified by performing IF on embryos (anti–LMN-1; a gift from Y. Gruenbaum; Fig. S2 A). Knockdown of SUN-1 was checked by performing IF on excised gonads using a phospho-SUN-1 antibody (gift of V. Jantsch, The Max F. Perutz Laboratory, Vienna, Austria). For GEI-17 and ZK1248.11, RNAi knockdown efficiency was confirmed by the generation of a sterile phenotype in a *set-25(n5021) met-2(n4256)* background.

Online supplemental materials

Fig. S1 shows that telomere FISH is specific. Fig. S2 shows that telomere anchoring is independent of H3 K9 methylation. Fig. S3 shows that telomere delocalization is not sufficient to induce large increases in telomeric C-circles. Table S1 describes the *C. elegans* strains used in this study. Online supplemental material is available at http://www.jcb.org/cgi/content/full/jcb.201307181/DC1. Additional data are available in the JCB DataViewer at http://dx.doi.org/10.1083/jcb.201307181.dv.

We'd like to thank the Caenorhabditis Genetics Center (University of Minnesota, Minneapolis, MN), Shawn Ahmed (University of North Carolina, Chapel Hill, NC), and Jan Karlseder (Salk Institute for Biological Studies, La Jolla, CA) for providing worm strains, and Shawn Ahmed for communicating unpublished results. We thank Yosef Gruenbaum and Verena Jantsch for providing antibodies. We also thank the FMI Facility for Advanced Imaging and Microscopy, I. Katic (Friedrich Miescher Institute [FMI], Basel, Switzerland), and Y. Gruenbaum for advice, and members of the Gasser and Ciosk laboratories at FMI for discussions.

The Gasser laboratory is supported by the Swiss National Science Foundation (31003A_138334), the Friedrich Miescher Institute for Biomedical Research, and the National Centers of Competence in Research Frontiers in Genetics.

Submitted: 29 July 2013
Accepted: 24 October 2013

References

Ahmed, S., and J. Hodgkin. 2000. MRT-2 checkpoint protein is required for germline immortality and telomere replication in *C. elegans*. *Nature*. 403:159–164. http://dx.doi.org/10.1038/35003120

Bao, Z., Z. Zhao, T.J. Boyle, J.I. Murray, and R.H. Waterston. 2008. Control of cell cycle timing during *C. elegans* embryogenesis. *Dev. Biol.* 318:65–72. http://dx.doi.org/10.1016/j.ydbio.2008.02.054

Bupp, J.M., A.E. Martin, E.S. Stensrud, and S.L. Jaspersen. 2007. Telomere anchoring at the nuclear periphery requires the budding yeast Sad1-UNC-84 domain protein Mps3. *J. Cell Biol.* 179:845–854. http://dx.doi.org/10.1083/jcb.200706040

Cheng, C., L. Shtessel, M.M. Brady, and S. Ahmed. 2012. *Caenorhabditis elegans* POT-2 telomere protein represses a mode of alternative lengthening of telomeres with normal telomere lengths. *Proc. Natl. Acad. Sci. USA*. 109:7805–7810. http://dx.doi.org/10.1073/pnas.1119191109

Cheung, I., M. Schertzer, A. Baross, A.M. Rose, P.M. Lansdorp, and D.M. Baird. 2004. Strain-specific telomere length revealed by single telomere length analysis in *Caenorhabditis elegans*. *Nucleic Acids Res.* 32:3383–3391. http://dx.doi.org/10.1093/nar/gkh661

Chung, H.M., C. Shea, S. Fields, R.N. Taub, L.H. Van der Ploeg, and D.B. Tse. 1990. Architectural organization in the interphase nucleus of the protozoan *Trypanosoma brucei*: location of telomeres and mini-chromosomes. *EMBO J.* 9:2611–2619.

Crabbe, L., A.J. Cesare, J.M. Kasuboski, J.A. Fitzpatrick, and J. Karlseder. 2012. Human telomeres are tethered to the nuclear envelope during postmitotic nuclear assembly. *Cell Rep.* 2:1521–1529. http://dx.doi.org/10.1016/j.celrep.2012.11.019

Dechat, T., K. Pfleghaar, K. Sengupta, T. Shimi, D.K. Shumaker, L. Solimando, and R.D. Goldman. 2008. Nuclear lamins: major factors in the structural organization and function of the nucleus and chromatin. *Genes Dev.* 22:832–853. http://dx.doi.org/10.1101/gad.1652708

de Lange, T. 2009. How telomeres solve the end-protection problem. *Science*. 326:948–952. http://dx.doi.org/10.1126/science.1170633

Draskovic, I., N. Arnoult, V. Steiner, S. Bacchetti, P. Lomonte, and A. Londoño-Vallejo. 2009. Probing PML body function in ALT cells reveals spatiotemporal requirements for telomere recombination. *Proc. Natl. Acad. Sci. USA*. 106:15726–15731. http://dx.doi.org/10.1073/pnas.0907689106

DuBois, K.N., S. Alsford, J.M. Holden, J. Buisson, M. Swiderski, J.M. Bart, A.V. Ratushny, Y. Wan, P. Bastin, J.D. Barry, et al. 2012. NUP-1 Is a large coiled-coil nucleoskeletal protein in trypanosomes with lamin-like functions. *PLoS Biol.* 10:e1001287. http://dx.doi.org/10.1371/journal.pbio.1001287

Ebrahimi, H., and A.D. Donaldson. 2008. Release of yeast telomeres from the nuclear periphery is triggered by replication and maintained by suppression

of Ku-mediated anchoring. *Genes Dev.* 22:3363–3374. http://dx.doi.org/10.1101/gad.486208

Ferreira, H.C., B. Luke, H. Schober, V. Kalck, J. Lingner, and S.M. Gasser. 2011. The PIAS homologue Siz2 regulates perinuclear telomere position and telomerase activity in budding yeast. *Nat. Cell Biol.* 13:867–874. http://dx.doi.org/10.1038/ncb2263

Funabiki, H., I. Hagan, S. Uzawa, and M. Yanagida. 1993. Cell cycle-dependent specific positioning and clustering of centromeres and telomeres in fission yeast. *J. Cell Biol.* 121:961–976. http://dx.doi.org/10.1083/jcb.121.5.961

Garvik, B., M. Carson, and L. Hartwell. 1995. Single-stranded DNA arising at telomeres in cdc13 mutants may constitute a specific signal for the RAD9 checkpoint. *Mol. Cell. Biol.* 15:6128–6138.

Gonzalez-Suarez, I., A.B. Redwood, S.M. Perkins, B. Vermolen, D. Lichtensztejin, D.A. Grotsky, L. Morgado-Palacin, E.J. Gapud, B.P. Sleckman, T. Sullivan, et al. 2009. Novel roles for A-type lamins in telomere biology and the DNA damage response pathway. *EMBO J.* 28:2414–2427. http://dx.doi.org/10.1038/emboj.2009.196

Gotta, M., T. Laroche, A. Formenton, L. Maillet, H. Scherthan, and S.M. Gasser. 1996. The clustering of telomeres and colocalization with Rap1, Sir3, and Sir4 proteins in wild-type *Saccharomyces cerevisiae*. *J. Cell Biol.* 134:1349–1363. http://dx.doi.org/10.1083/jcb.134.6.1349

Hagelstrom, R.T., K.B. Blagoev, L.J. Niedernhofer, E.H. Goodwin, and S.M. Bailey. 2010. Hyper telomere recombination accelerates replicative senescence and may promote premature aging. *Proc. Natl. Acad. Sci. USA*. 107:15768–15773. http://dx.doi.org/10.1073/pnas.1006338107

Henson, J.D., Y. Cao, L.I. Huschtscha, A.C. Chang, A.Y. Au, H.A. Pickett, and R.R. Reddel. 2009. DNA C-circles are specific and quantifiable markers of alternative-lengthening-of-telomeres activity. *Nat. Biotechnol.* 27:1181–1185. http://dx.doi.org/10.1038/nbt.1587

Horn, H.F., Z. Brownstein, D.R. Lenz, S. Shivatzki, A.A. Dror, O. Dagan-Rosenfeld, L.M. Friedman, K.J. Roux, S. Kozlov, K.T. Jeang, et al. 2013. The LINC complex is essential for hearing. *J. Clin. Invest.* 123:740–750. http://dx.doi.org/10.1172/JCI66911

Jegou, T., I. Chung, G. Heuvelman, M. Wachsmuth, S.M. Görisch, K.M. Greulich-Bode, P. Boukamp, P. Lichter, and K. Rippe. 2009. Dynamics of telomeres and promyelocytic leukemia nuclear bodies in a telomerase-negative human cell line. *Mol. Biol. Cell*. 20:2070–2082. http://dx.doi.org/10.1091/mbc.E08-02-0108

Lackner, D.H., M. Raices, H. Maruyama, C. Haggblom, and J. Karlseder. 2012. Organismal propagation in the absence of a functional telomerase pathway in *Caenorhabditis elegans*. *EMBO J.* 31:2024–2033. http://dx.doi.org/10.1038/emboj.2012.61

Laroche, T., S.G. Martin, M. Gotta, H.C. Gorham, F.E. Pryde, E.J. Louis, and S.M. Gasser. 1998. Mutation of yeast Ku genes disrupts the subnuclear organization of telomeres. *Curr. Biol.* 8:653–656. http://dx.doi.org/10.1016/S0960-9822(98)70252-0

Liu, T., A. Rechtsteiner, T.A. Egelhofer, A. Vielle, I. Latorre, M.S. Cheung, S. Ercan, K. Ikegami, M. Jensen, P. Kolasinska-Zwierz, et al. 2011. Broad chromosomal domains of histone modification patterns in *C. elegans*. *Genome Res.* 21:227–236. http://dx.doi.org/10.1101/gr.115519.110

Lowden, M.R., B. Meier, T.W. Lee, J. Hall, and S. Ahmed. 2008. End joining at *Caenorhabditis elegans* telomeres. *Genetics*. 180:741–754. http://dx.doi.org/10.1534/genetics.108.089920

Marshall, W.F., A.F. Dernburg, B. Harmon, D.A. Agard, and J.W. Sedat. 1996. Specific interactions of chromatin with the nuclear envelope: positional determination within the nucleus in *Drosophila melanogaster*. *Mol. Biol. Cell*. 7:825–842. http://dx.doi.org/10.1091/mbc.7.5.825

Mattout, A., B.L. Pike, B.D. Towbin, E.M. Bank, A. Gonzalez-Sandoval, M.B. Stadler, P. Meister, Y. Gruenbaum, and S.M. Gasser. 2011. An EDMD mutation in *C. elegans* lamin blocks muscle-specific gene relocation and compromises muscle integrity. *Curr. Biol.* 21:1603–1614. http://dx.doi.org/10.1016/j.cub.2011.08.030

Meier, B., I. Clejan, Y. Liu, M. Lowden, A. Gartner, J. Hodgkin, and S. Ahmed. 2006. trt-1 is the *Caenorhabditis elegans* catalytic subunit of telomerase. *PLoS Genet.* 2:e18. http://dx.doi.org/10.1371/journal.pgen.0020018

Meister, P., L.R. Gehlen, E. Varela, V. Kalck, and S.M. Gasser. 2010a. Visualizing yeast chromosomes and nuclear architecture. *Methods Enzymol.* 470:535–567. http://dx.doi.org/10.1016/S0076-6879(10)70021-5

Meister, P., B.D. Towbin, B.L. Pike, A. Ponti, and S.M. Gasser. 2010b. The spatial dynamics of tissue-specific promoters during *C. elegans* development. *Genes Dev.* 24:766–782. http://dx.doi.org/10.1101/gad.559610

Nagai, S., P. Heun, and S.M. Gasser. 2010. Roles for nuclear organization in the maintenance of genome stability. *Epigenomics*. 2:289–305. http://dx.doi.org/10.2217/epi.09.49

Nagele, R.G., A.Q. Velasco, W.J. Anderson, D.J. McMahon, Z. Thomson, J. Fazekas, K. Wind, and H. Lee. 2001. Telomere associations in interphase nuclei: possible role in maintenance of interphase chromosome topology. *J. Cell Sci.* 114:377–388.

Palladino, F., T. Laroche, E. Gilson, A. Axelrod, L. Pillus, and S.M. Gasser. 1993. SIR3 and SIR4 proteins are required for the positioning and integrity of yeast telomeres. *Cell*. 75:543–555. http://dx.doi.org/10.1016/0092-8674(93)90388-7

Penkner, A., L. Tang, M. Novatchkova, M. Ladurner, A. Fridkin, Y. Gruenbaum, D. Schweizer, J. Loidl, and V. Jantsch. 2007. The nuclear envelope protein Matefin/SUN-1 is required for homologous pairing in *C. elegans* meiosis. *Dev. Cell*. 12:873–885. http://dx.doi.org/10.1016/j.devcel.2007.05.004

Potts, P.R., and H. Yu. 2007. The SMC5/6 complex maintains telomere length in ALT cancer cells through SUMOylation of telomere-binding proteins. *Nat. Struct. Mol. Biol.* 14:581–590. http://dx.doi.org/10.1038/nsmb1259

Raices, M., R.E. Verdun, S.A. Compton, C.I. Haggblom, J.D. Griffith, A. Dillin, and J. Karlseder. 2008. *C. elegans* telomeres contain G-strand and C-strand overhangs that are bound by distinct proteins. *Cell*. 132:745–757. http://dx.doi.org/10.1016/j.cell.2007.12.039

Rawlins, D.J., and P.J. Shaw. 1990. Localization of ribosomal and telomeric DNA sequences in intact plant nuclei by in-situ hybridization and three-dimensional optical microscopy. *J. Microsc.* 157:83–89. http://dx.doi.org/10.1111/j.1365-2818.1990.tb02949.x

Schober, H., H. Ferreira, V. Kalck, L.R. Gehlen, and S.M. Gasser. 2009. Yeast telomerase and the SUN domain protein Mps3 anchor telomeres and repress subtelomeric recombination. *Genes Dev.* 23:928–938. http://dx.doi.org/10.1101/gad.1787509

Shtessel, L., M.R. Lowden, C. Cheng, M. Simon, K. Wang, and S. Ahmed. 2013. *Caenorhabditis elegans* POT-1 and POT-2 repress telomere maintenance pathways. *G3 (Bethesda)*. 3:305–313. http://dx.doi.org/10.1534/g3.112.004440

Starr, D.A. 2009. A nuclear-envelope bridge positions nuclei and moves chromosomes. *J. Cell Sci.* 122:577–586. http://dx.doi.org/10.1242/jcs.037622

Szostak, J.W., and E.H. Blackburn. 1982. Cloning yeast telomeres on linear plasmid vectors. *Cell*. 29:245–255. http://dx.doi.org/10.1016/0092-8674(82)90109-X

Taddei, A., G. Van Houwe, S. Nagai, I. Erb, E. van Nimwegen, and S.M. Gasser. 2009. The functional importance of telomere clustering: global changes in gene expression result from SIR factor dispersion. *Genome Res.* 19:611–625. http://dx.doi.org/10.1101/gr.083881.108

Timmons, L., D.L. Court, and A. Fire. 2001. Ingestion of bacterially expressed dsRNAs can produce specific and potent genetic interference in *Caenorhabditis elegans*. *Gene*. 263:103–112. http://dx.doi.org/10.1016/S0378-1119(00)00579-5

Towbin, B.D., C. González-Aguilera, R. Sack, D. Gaidatzis, V. Kalck, P. Meister, P. Askjaer, and S.M. Gasser. 2012. Step-wise methylation of histone H3K9 positions heterochromatin at the nuclear periphery. *Cell*. 150:934–947. http://dx.doi.org/10.1016/j.cell.2012.06.051

Vannier, J.B., V. Pavicic-Kaltenbrunner, M.I. Petalcorin, H. Ding, and S.J. Boulton. 2012. RTEL1 dismantles T loops and counteracts telomeric G4-DNA to maintain telomere integrity. *Cell*. 149:795–806. http://dx.doi.org/10.1016/j.cell.2012.03.030

Wellinger, R.J., A.J. Wolf, and V.A. Zakian. 1993. *Saccharomyces* telomeres acquire single-strand TG1-3 tails late in S phase. *Cell*. 72:51–60. http://dx.doi.org/10.1016/0092-8674(93)90049-V

Wright, W.E., V.M. Tesmer, K.E. Huffman, S.D. Levene, and J.W. Shay. 1997. Normal human chromosomes have long G-rich telomeric overhangs at one end. *Genes Dev.* 11:2801–2809. http://dx.doi.org/10.1101/gad.11.21.2801

Yeager, T.R., A.A. Neumann, A. Englezou, L.I. Huschtscha, J.R. Noble, and R.R. Reddel. 1999. Telomerase-negative immortalized human cells contain a novel type of promyelocytic leukemia (PML) body. *Cancer Res.* 59:4175–4179.